ON THE EFFECT OF RESIDUAL INTERFEROMETER ABERRATION ON THE QUALITY OF INTERFEROMETRIC MEASUREMENTS

I.G. Polovtsev and G.V. Simonova

Special Design Bureau "Optika",
Siberian Branch of the Academy of Sciences of the USSR, Tomsk
Received July 18, 1989

Various interferometer schemes are analyzed from the view point of the effect of the residual aberrations on the accuracy of interference measurements. It is shown that this factor is important and recommendations are made for the setting the tolerances for the optical components of the interferometers.

Interference measurements are very often used both in various problems of optical sounding of the atmosphere and in fabricating the optical components for lidar systems.

In interferometry the quality of the interferometric wavefronts is usually evaluated visually. The development of methods for automatic processing of interferograms has opened up the possibility of obtaining information about the quality of the monitored wave surfaces with extremely low error of $\lambda/100$ from the amplitude of the error (the reproducibility of the results).[1] But interference measurements are significantly affected by the residual interferometer aberrations, produced by the optics of the instrument. This error is a systematic error and can be accounted for by digital correction.

For example, a well-known "MARK-II" interferometer[1] has a monitoring error of $\lambda/20$ for flat and $\lambda/10$ for spherical wavefronts. The "MARK-III" interferometer, which has the same optical layout but is equipped with a digital correction system, has an error of $\lambda/50$. It should be noted that the residual interferometer aberration and the error of interference measurements are two different concepts, since the interference pattern characterizes the difference of the wavefronts in the two arms of the interferometer. Therefore if residual aberration is present, the question of the optical path in the different arms of the interferometer becomes very important.

It was shown in Ref. 2 that the wave aberration N of a spherical wavefront of radius R acquires at a distance ΔR an increment ΔN, given by the relation

$$|\Delta N| = \left|\frac{R\,\Delta R}{2(R-\Delta R)}\right|\varphi^2,$$

where φ is the tilt angle of the wavefront normal. In Ref. 3 it is shown the maximum tilt angle of the normal φ_{max} can be determined from the relation

$$\varphi_{max} \simeq kN_{max}/D,$$

where D is the wavefront diameter; k is the coefficient determined by the specific form of wave aberration; and, N_{max} is the maximum wave aberration at an inner diameter. It follows from the above that the maximum variation of wave aberration is

$$|\Delta N_{max}| \simeq \begin{cases} k_{sph}^2 \dfrac{|R\,\Delta R|}{2|R-\Delta R|}\left[\dfrac{N_{max}}{D}\right]^2 & \text{for a spherical wavefront} \\ k_f^2 \dfrac{|\Delta R|}{2}\left[\dfrac{N_{max}}{D}\right]^2 & \text{for a flat wavefront} \end{cases} \qquad (1)$$

The coefficients k_{sph} and k_f can be determined by a computational method. Let ΔR be the difference between the optical paths in the arms of the interferometer, ΔN_{max} the maximum systematic error in the interference measurements for an instrument, whose residual aberration in the reference plane is N_{max}, D the inner diameter of the reference surface; and, R the radius of curvature of the reference front. Then the relation (1) shows that both the residual aberrations and the geometry of the scheme significantly affect the measurements.

In Ref. 4 it is shown that the effect of the length of the working arm of the Twyiman-Green interferometer (Fig. 1a) in the presence of residual aberration is small $\Delta N \ll N$ but significant for precision measurements on long paths.

By a simple technical means[4] the effect of the residual aberration on the quality of the interferometric contrast can be significantly reduced. In the process the error does not exceed $\lambda/90$. The Twyiman-Green scheme nonetheless can hardly be considered acceptable for high-precision measurements, since it contains a large number of surfaces, the error in the formation of which affects even more strongly the results of monitoring, so that they must be formed with very high quality. In Fig. 1a these are the surfaces A and B and the surface of the reference mirror. All other surfaces are common, and they affect the result through the residual aberration.

0235-6880/90/06 605-06 $02.00

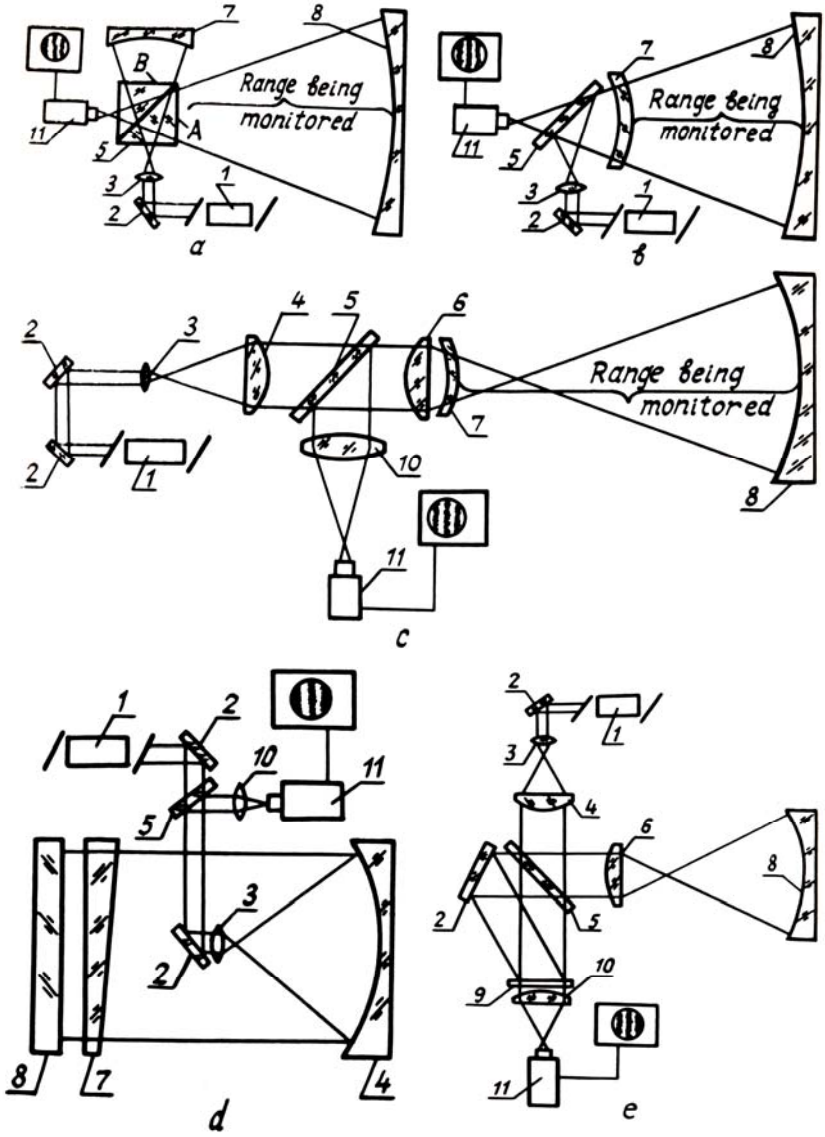

FIG. 1. Interferometer schemes: a) a Twyiman-Green interferometer for monitoring concave spherical surfaces; b) converging-beam interferometer for monitoring concave spherical surfaces; c) diverging-beam interferometer for monitoring both convex and concave spherical mirrors; d) parallel-beam interferometer for monitoring flat surfaces; e) holographic interferometer for monitoring convex and concave spherical mirrors. 1) laser; 2) aiming mirrors; 3) microobjective; 4) collimating objective (mirror); 5) beamsplitter; 6) forming objective; 7) optical element with reference surface (reference mirror, aplanatic meniscus lens wedge); 8) surface being monitored; 9) hologram; 10) converging objective; 11) TV camera with video control unit.

From this standpoint interferometers with coincident arms are better. Figure 1b shows a conversing-beam interferometer (CBI). Figure 1c shows a divergent-beam interferometer (DBI), and Figure 1d shows a parallel-beam interferometer (PBI), the so-called Fizeau interferometer.

The optical arrangement of the CBI permits working with both convex and concave surfaces. In contrast to the interferometer shown in Fig. 1a, all components are common and the meniscus lens 7 with a standard back surface is aplanatic. Nonetheless because there are so many optical elements (see positions 3–7 in Fig. 1b) in the common part of the CBI quite stringent requirements must be imposed on the quality of the optical components. Table I gives the results of numerical calculation, performed on a computer for a CBI with the following parameters:

– the inner diameter of the beam-splitting meniscus lens 7 $D = 30$ mm;

– the radius of curvature for the reference wavefront $R = 32.73$ mm.

Wave aberration was modeled by varying the eccentricity of one component of the objective 6. The average value

$$\bar{k}^2_{sph} \simeq 310,$$

was obtained from the data in ΔN_{cal} in the first column of Table I and the values of ΔN_{th} were calculated from relation (1). The results agree quite well with one another. When the relation (1) is used the error ΔN of the estimate does not exceed 50%. It should also be noted that the error of this estimate increases as the caustic is approached.[2]

TABLE I.

Effect of residual aberration N and CBI path difference ΔR on the monitoring error. ΔN_{cal}, are the errors determined by direct numerical calculation and ΔN_{th} are the errors determined from the relation (1).

ΔR, mm	N, μm					
	2.72		0.857		4.062	
	ΔN_c	ΔN_t	ΔN_c	ΔN_t	ΔN_c	ΔN_t
1032.73	1.030	0.043	0.004	0.0043	0.089	0.1
132.73	0.053	0.055	0.005	0.0054	0.122	0.123
62.73	0.093	0.087	0.009	0.009	0.214	0.19
37.73	0.565	0.31	0.057	0.03	1.324	0.7
22.73	0.045	0.09	0.005	0.009	0.105	0.2
2.73	0.003	0.004	0.0002	0.0003	0.005	0.009

If $\Delta R = R$, i.e., when the surface being monitored is placed at the caustic, the relation (1) has a singularity and the difference between the wave aberrations becomes maximal. From here it follows that the residual aberration of the CBI can be easily controlled. For this it is sufficient to place any optical surface at the caustic.

The relation (1) may be used to determine the manufacturing tolerances for the optical components. For example, to achieve high-quality monitoring of surfaces whose radius of curvature is not less than 5 mm with a systematic error not exceeding $\lambda/20$ in the described interferometer the residual aberration N_{max} must satisfy the relation (taking into account the error (1)):

$$|N_{max}| \leq 0.5 \sqrt{\left|\frac{\Delta N_{max} \cdot D^2 \cdot 2(R - \Delta R)}{R \cdot \Delta R \cdot 310}\right|} = 0.5 \text{ μm}.$$

The stringent restrictions imposed on the residual aberration lead to stringent manufacturing tolerances for the beamsplitting meniscus lens. For example, for a meniscus lens 7 with the parameters $r_1 = 23.33$, $r_2 = 32.73$, $d = 6$, $\varnothing = 28$ mm, $n = 1.5147$ the tolerances are $\Delta r_{1,2} = \pm 0.008$ mm, $\Delta d = \pm 0.01$ mm, and $\Delta n = \pm 0.0001$.

The divergent-beam interferometer (DBI) has considerably fewer optical components (positions 3, 5, 7 in Fig. 1c) in its illuminating part. When a point filtration device is introduced only the surface of the mirror 5 and the meniscus lens 7 remain. Therefore if a convergent beam is not necessary the DBI technique becomes preferable. To set the manufacturing tolerances for the optical components one the relation (1) can be employed by analogy to the CBI with at $k^2_{sph} = 310$.

The Fizeau interferometer scheme (Fig. 1d) (PBI) is widely used for monitoring the quality of flat surfaces. The distance between the reference and the monitored surfaces is usually made as short as much as possible, so as to reduce to a minimum the effect of residual aberration and adjustment errors. Actually the PBI scheme permits a significant path difference with considerable residual aberration. This is extremely important for measurements with long paths.

Table II presents the results of a numerical calculation for a PBI with an aperture diameter $D = 300$ m. The wave aberration N was modeled by changing eccentricity of one of the components of the optical scheme. The average value

$$\bar{k}^2_f \simeq 94,$$

was obtained from the data on ΔN_{cal} in the first column of Table II and the values of ΔN_{th} were calculated using the relation (1). The obtained results agree quite well with one another. The estimation error ΔN obtained using the relation (1) does not exceed 50%.

The relation (1) shows that to achieve high-quality monitoring with a systematic error not exceeding $\lambda/20$ and a path difference of 1–1000 mm the residual aberration must be corrected to (taking into account the estimate (1))

$$N_{max} \leq 0.5 \sqrt{\frac{\Delta N_{max} \cdot 2D^2}{\Delta R \cdot 94}} = 3.9 \text{ μm}.$$

In case the path difference is 1000-8000 mm, $N_{max} < 1.5$ μm. For short paths, up to 100 mm, $N_{max} \leq 12.3$ μm. Note, however, that these estimates of the residual aberration include a restriction on the beam focusing, so that the residual aberration of the PBI may be quite large. If in it the alignment at infinity is very precise.

TABLE II.

The effect of residual aberration N and path difference ΔR in a PBI on the monitoring error. ΔN_{cal} is the error obtained by direct calculation and ΔN_{th} in the error obtained from the relation (11).

ΔR, mm	N, μm					
	5.75		10.56		15.68	
	ΔN_c	ΔN_t	ΔN_c	ΔN_t	ΔN_c	ΔN_t
1	$0.1 \cdot 10^{-4}$	$0.17 \cdot 10^{-4}$	$0.7 \cdot 10^{-4}$	$0.57 \cdot 10^{-7}$	$0.26 \cdot 10^{-3}$	$0.13 \cdot 10^{-3}$
5	$0.4 \cdot 10^{-4}$	$0.85 \cdot 10^{-4}$	$0.4 \cdot 10^{-3}$	$0.3 \cdot 10^{-3}$	$0.12 \cdot 10^{-2}$	$0.65 \cdot 10^{-3}$
10	$0.13 \cdot 10^{-3}$	$0.17 \cdot 10^{-3}$	$0.8 \cdot 10^{-3}$	$0.57 \cdot 10^{-3}$	$0.24 \cdot 10^{-2}$	$0.13 \cdot 10^{-2}$
15	$0.25 \cdot 10^{-3}$	$0.26 \cdot 10^{-3}$	$0.12 \cdot 10^{-2}$	$0.87 \cdot 10^{-3}$	$0.37 \cdot 10^{-2}$	$0.2 \cdot 10^{-2}$
20	$0.34 \cdot 10^{-3}$	$0.34 \cdot 10^{-3}$	$0.16 \cdot 10^{-2}$	$0.11 \cdot 10^{-2}$	$0.49 \cdot 10^{-2}$	$0.26 \cdot 10^{-2}$
50	$0.84 \cdot 10^{-3}$	$0.85 \cdot 10^{-3}$	$0.25 \cdot 10^{-2}$	$0.29 \cdot 10^{-2}$	$0.12 \cdot 10^{-1}$	$0.6 \cdot 10^{-2}$
100	$0.17 \cdot 10^{-2}$	$0.17 \cdot 10^{-2}$	$0.41 \cdot 10^{-2}$	$0.57 \cdot 10^{-2}$	$0.24 \cdot 10^{-1}$	$0.13 \cdot 10^{-1}$
1000	$0.17 \cdot 10^{-1}$	$0.17 \cdot 10^{-1}$	$0.82 \cdot 10^{-1}$	$0.57 \cdot 10^{-1}$	0.24	0.13
8000	0.12	0.14	0.59	0.47	1.72	1

A holographic interferometer (HI) cam be constructed for any of the schemes described above. Figure 1e shows an example of an analog of a the CBI with holographic correction of the residual aberration (RA).

A wide laser beam from the objective of the collimator (4) is split into working and reference beams. The working beam is passes into an photographic objective 6, whose focal point is above the center of curvature of the reference sphere 8, and the reference beam passes to the mirror 2. After reflection both beams meet on the photographic plate 9, where the interfering light waves are holographically recorded. If after exposure and chemical processing the plate (hologram) is placed at its former position, then two interference patterns can be observed behind the hologram in the direction of the working and reference beams.

During actual monitoring the test object is inserted instead of a standard object. The surface errors are judged from the shape of the observed interference fringes, as done in the standard interferometers. Here the wavefront constructed from the hologram plays the role of the reference wavefront. Obviously, when the radius of the test object is equal to that of standard object, the correction of the RA is performed absolutely (with accuracy up to wavefront errors introduced by the processing of the hologram). But, based on what was said above, when the radius of the test object changes the effect of RA will increase. For this reason, in an HI the RA should be a corrected with the help of a sufficiently large number of standards.

Another feature of an HI is that the hologram must be positioned extremely precisely. Any misalignment results in a considerable increase in the residual aberration. The tolerances on the RA is HI can be calculated using the relation (1).

The following conclusions, which should be kept in mind when designing interferometers and choosing a scheme, can be drawn based on what was said above:

– a high-quality interferometer is one in which the monitoring error does not exceed λ/20 with respect to the amplitude of the error;

– interferometers with coincident arms are best for high-quality interference measurements;

– the problem of constructing a high- precision interferometer is quite complicated and requires high-quality optical components in all parts of the interferometer; in addition, in each specific case the overall design should be simplified as must as possible, even at the loss of universality;

–to perform calculations and to set the manufacturing tolerances for the optical components and also to estimate the systematic error of the interferometer the following relation can be used

$$\Delta N = \begin{cases} 310 \dfrac{R\,\Delta R}{2(R-\Delta R)} - \left[\dfrac{N_{max}}{D}\right]^2 - & \text{for a spherical wavefront;} \\ 94 \dfrac{\Delta R}{2}\left[\dfrac{N_{max}}{D}\right]^2 - & \text{for a flat wavefront.} \end{cases} \quad (2)$$

REFERENCES

1. *Measuring instruments for quality control in the optical industry,* ORIEL Advertisement Booklet.
2. D.T. Puryaev, in: *Techniques for Monitoring Aspherical Optical Surfaces* (in Russian) Mashinostroyenie, Moscow (1976), pp. 110–111.
3. I.G. Polovtsev, Atmos. Opt. **2**, No. 4., 307–312 (1989).
4. I.G. Polovtsev and G.V. Simonova, Atmos. Opt. **2**, No. 5. 430–433 (1989).
5. *The Optical Technologist's Handbook* [in Russian], Mashinostroenie, Leningrad (1983), 321.
6. I.I. Dukhopel and L.G. Fedina, Opt.-Mekh. Prom.-st'. No. 8, 50–58 (1973).
7. T.S. Kolomiitseva and L.G. Fedina, Opt.-Mekh. Prom.-st', No. 2. 32–35 (1976).